HHS Public Access

Author manuscript

Eur J Neurosci. Author manuscript; available in PMC 2019 May 01.

Published in final edited form as:

Eur J Neurosci. 2018 May ; 47(10): 1208–1218. doi:10.1111/ejn.13879.

Synaptic function and plasticity in identified inhibitory inputs onto VTA dopamine neurons

Abigail M. Polter[1,2,3], **Kelsey Barcomb**[1,3], **Ayumi C. Tsuda**[1], and **Julie A. Kauer**[1,*]

[1]Brown University, Department of Molecular Pharmacology, Physiology and Biotechnology Providence, RI 02912

[2]current address: George Washington University, Department of Pharmacology and Physiology, Washington, DC 20037

[3]contributed equally

Abstract

Ventral tegmental area (VTA) dopaminergic neurons are key components of the reward pathway, and their activity is powerfully controlled by a diverse array of inhibitory GABAergic inputs. Two major sources of GABAergic nerve terminals within the VTA are local VTA interneurons and neurons in the rostromedial tegmental nucleus (RMTg). Here, using optogenetics, we compared synaptic properties of GABAergic synapses on VTA dopamine neurons using selective activation of afferents that originate from these two cell populations. We found little evidence of co-release of glutamate from either input, but RMTg-originating synaptic currents were reduced by strychnine, suggesting co-release of glycine and GABA. VTA- originating synapses displayed a lower initial release probability, and at higher frequency stimulation, short-term depression was more marked in VTA- but not RMTg-originating synapses. We previously reported that nitric oxide (NO)-induced potentiation of GABAergic synapses on VTA dopaminergic cells is lost after exposure to drugs of abuse or acute stress; in these experiments, multiple GABAergic afferents were simultaneously activated by electrical stimulation. Here we found that optogenetically-activated VTA-originating synapses on presumptive dopamine neurons also exhibited NO-induced potentiation, whereas RMTg- originating synapses did not. Despite providing a robust inhibitory input to the VTA, RMTg GABAergic synapses are most likely not those previously shown by our work to be persistently altered by addictive drugs and stress. Our work emphasizes the idea that dopamine neuron excitability is controlled by diverse inhibitory inputs expected to exert varying degrees of inhibition and to participate differently in a range of behaviors.

*Corresponding Author: Julie Kauer, Ph.D., Brown University, Department of Molecular Pharmacology, Physiology and Biotechnology, 171 Meeting St., Box G-B3, Providence, RI 02912, Phone: (401) 863-9803, Julie_Kauer@brown.edu.

Author Contributions

AMP and KB performed all electrophysiology experiments and analyzed data. ACT performed immunohistochemistry, confocal imaging, and stereotaxic surgeries. AMP and JAK conceived and designed the study and drafted the manuscript. KB edited the manuscript. All authors have read and approved the final version of the manuscript.

Conflict of Interest

All authors confirm that they have no conflicts of interest.

Data Accountability

All original data are available upon request.

Keywords

GABAergic circuits; RMTg; optogenetics; LTP

Introduction

Dopamine neurons in the ventral tegmental area (VTA) are critical to the encoding of rewarding and aversive stimuli and are required for addiction to drugs of abuse (Lammel *et al.*, 2014; Holly & Miczek, 2016; Morales & Margolis, 2017). Inhibitory and excitatory synaptic inputs change the activity of dopamine neurons in response to environmental stimuli, either by altering the firing rate or by shifting the neuron from a tonic to phasic firing pattern (Suaud-Chagny et al., 1992; Chergui et al., 1993; Mereu et al., 1997). Dopamine neurons are relatively depolarized basally and are spontaneously active both in vivo and in brain slices. $GABA_AR$ synapses interrupt dopaminergic cell firing both by hyperpolarization and by increasing conductance (Paladini *et al.*, 1999a; Paladini *et al.*, 1999b; Tan *et al.*, 2012; Van Zessen *et al.*, 2012), reducing the firing rate of dopamine neurons as shown in both pharmacological (Johnson & North, 1992; Suaud-Chagny *et al.*, 1992; Paladini *et al.*, 1999b) and optogenetic studies (Tan et al., 2012; Van Zessen et al., 2012; Simmons et al., 2017). Inhibitory synapses in the VTA are also dynamically regulated by experience. For example, plasticity of inhibitory synapses is lost or altered after exposure to morphine (Nugent *et al.*, 2007; Niehaus *et al.*, 2010; Matsui & Williams, 2011; Graziane *et al.*, 2013; Matsui *et al.*, 2014; Baimel & Borgland, 2015), cocaine (Liu *et al.*, 2005; Niehaus *et al.*, 2010), and alcohol (Melis *et al.*, 2002; Guan & Ye, 2010), or following stressful experiences (Niehaus *et al.*, 2010; Graziane *et al.*, 2013; Polter *et al.*, 2014, 2017; Authement *et al.*, 2015; Ostroumov *et al.*, 2016).

Local VTA GABAergic neurons comprise approximately 35% of cells in the VTA (Nair-Roberts *et al.*, 2008; Taylor *et al.*, 2014) and form inhibitory synapses onto VTA dopaminergic neurons (Omelchenko and Sesack, 2009a; Tan et al., 2012; Van Zessen et al., 2012; Matsui et al., 2014; Simmons et al., 2017). However, dopamine neurons also receive long-range inhibitory inputs from the rostromedial tegmental nucleus (RMTg, also known as the tail of the VTA; Jhou et al., 2009a; Matsui and Williams, 2011; Lammel et al., 2012; Lecca et al., 2012; Stamatakis and Stuber, 2012; Matsui et al., 2014; Kaufling and Aston-Jones, 2015; Simmons et al., 2017), the ventral pallidum (Haber *et al.*, 1985; Hjelmstad *et al.*, 2013), the bed nucleus of the stria terminalis (BNST) (Jennings *et al.*, 2013), and the nucleus accumbens (Xia et al., 2011; Bocklisch et al., 2013; Edwards et al., 2017; Simmons et al., 2017), as well as from more caudal brain regions (Omelchenko & Sesack, 2010; Sharpe *et al.*, 2017). Inhibitory synapses arising from each of these brain regions are likely to have distinct functional circuit roles and to be differentially regulated by experience.

Through their modulation of VTA dopamine neuron activity, GABAergic afferents from both the RMTg and the VTA play a significant role in reward and aversion (Bourdy and Barrot, 2012; Tan et al., 2012; Van Zessen et al. 2012; Creed et al., 2014; Jhou et al., 2013; Vento et al., 2017). Despite recent advances in understanding the circuitry and behavioral relevance of inhibition in the ventral tegmental area, there are relatively few studies taking

advantage of modern tools to probe VTA dopamine neuron regulation by distinct sources of inhibition. Here, we report that RMTg- and VTA-originating inhibitory synapses exhibit differing basal synaptic properties and short-term plasticity during trains of presynaptic action potentials. VTA but not RMTg inhibitory synapses also express nitric oxide-dependent long-term potentiation (LTP_{GABA}).

Materials and Methods

Animals:

All procedures were carried out in accordance with the guidelines of the National Institutes of Health for animal care and use and were approved by the Brown University Institutional Animal Care and Use Committee. VGAT-Cre mice (Vong *et al.*, 2011; Jackson labs, Bar Harbor, ME) were used for all studies. Homozygous pairs were continuously bred in-house at Brown University, where they were maintained on a 12-h light/dark cycle and provided food and water *ad libitum*. **A total of 52 mice were used for electrophysiological experiments and 4 for immunohistochemistry**.

Stereotaxic injection of virus:

Intracranial injection of virus was performed at P25–29 on male mice. Mice were deeply anesthetized with ketamine (75 mg/kg) and dexmedetomidine (0.25mg/kg) and then 200–300 nL of AAV2-EF1a-DIO-hChR2(H134R)-EYFP (6.4×10e11 molecules/ml) or AAV-EF1a-DIO-hChR2(H134R)-mCherry (1.3×10e12 molecules/ml) (UNC vector core) was injected into the RMTg (AP:−2.5, ML: ±0.5 DV:−4.4) or VTA (AP:−1.7, ML: ±0.75, DV: −4.5). Mice were singly housed post-surgery and allowed to recover for 18–28 days before further experimentation to allow for optimal expression of virus.

Immunohistochemistry and Imaging

Mice were deeply anesthetized with an intraperitoneal injection of ketamine (75 mg/kg) and dexmedetomidine (0.25mg/kg) and transcardially perfused with PBS followed by 4% PFA. Whole brains were removed and post-fixed overnight in 4% PFA, then dehydrated in 30% sucrose. Using a vibratome, 50 μm coronal sections were collected in PBS. For immunostaining, free floating slices were washed in warmed PBS containing 5% Triton-X 100 (PBS-T), and blocked in 5% normal donkey serum (NDS) and 5% bovine serum albumin (BSA) in PBS. Sections were then incubated in primary antibody against tyrosine hydroxylase (Millipore AB152, 1:1000) or FoxP1 (Abcam ab16645, 1:20,000) in 0.1% PBS-T at 4°C. Sections were washed in PBS, blocked in 5% NDS in 0.25% PBS-T for three washes (10 min), then incubated in secondary antibodies (donkey anti-rabbit conjugated to Alexa-594 or Alexa-405 fluorescent dyes, ThermoFisher, **1:500 for tyrosine hydroxylase, 1:1000 for FoxP1**) for 3 hours at room temperature. Slices were rinsed in PBS and then mounted on slides with Fluoromount-G mounting medium (Southern Biotech).

Imaging of immunofluorescence and virally expressed fluorescent proteins was performed using a Zeiss LSM 800 with 10x, 20x, and 40x (water immersion) objectives. eYFP was imaged using a 488 nm diode laser; Alexa594 and RFP were imaged using a 561 nm diode laser; and Alexa 405 was imaged using the 405 diode laser. 40x images represent projections

of 15–25 z-stacks using 1.03 micron step size over 15–20 microns; 4x images represent single optical planes 2 microns thick (Voxel size 40X: 0.0243 μm^3, 20X: 0.3972 μm^3). Images were processed and analyzed using Zeiss Zen Blue software and Adobe Illustrator CC 2017.

Preparation of brain slices:

Slices were prepared from deeply anesthetized mice perfused with ice-cold NMDG ringer (in mM): 92 NMDG, 2.5 KCl, 1.2 NaH_2PO_4, 30 $NaHCO_3$, 20 HEPES, 25 glucose, 5 sodium ascorbate, 2 thiourea, 3 sodium pyruvate, 10 $MgSO_4$, 0.5 $CaCl_2$ (Ting *et al.*, 2014). Following perfusion, the brain was rapidly dissected and coronal slices (220 μm) were prepared in NMDG ringer using a vibratome. Sections from both the VTA and RMTg were collected from all animals to confirm accurate targeting of the viral injection site. Slices recovered for 1 h at 34°C in oxygenated HEPES holding solution (in mM): 86 NaCl, 2.5 KCl, 1.2 NaH_2PO_4, 35 $NaHCO_3$, 20 HEPES, 25 glucose, 5 sodium ascorbate, 2 thiourea, 3 sodium pyruvate, 1 $MgSO_4$, 2 $CaCl_2$ (Ting *et al.*, 2014), and then were held in the same solution at room temperature until use.

Electrophysiology:

General methods were as previously reported (Niehaus *et al.*, 2009; Polter *et al.*, 2014). Midbrain slices were continuously perfused at 1.5–2 mL / min with ACSF (28–32°C) containing (in mM): 126 NaCl, 21.4 $NaHCO_3$, 2.5 KCl, 1.2 NaH_2PO_4, 2.4 $CaCl_2$, 1.0 $MgSO_4$, 11.1 glucose. Patch pipettes were filled with (in mM): 125 KCl, 2.8 NaCl, 2 $MgCl_2$, 2 ATP-Na+, 0.3 GTP-Na+, 0.6 EGTA, and 10 HEPES. Unless otherwise indicated, the cells included in this study were selected based on the presence of an I_h (> 25 pA) during a voltage step from −50 mV to - 100 mV; such cells are likely dopaminergic (Ungless & Grace, 2012; Baimel *et al.*, 2017; Edwards *et al.*, 2017).

Channelrhodopsin-expressing cells were identified visually by eYFP fluorescence and electrophysiologically by the presence of a persistent inward current response to a 150 ms light pulse. Channelrhodopsin-induced action potentials were recorded in current clamp from these cells using a 0.4–4 ms light pulse at 20 Hz. To record channelrhodopsin-induced synaptic currents, non-fluorescent cells were voltage-clamped at −70 mV and currents were evoked using 0.4–4 ms light pulses delivered through the microscope objective from a white LED (Mightex) controlled by an LED driver (LEDD1B, ThorLabs). On this device the duty cycle range is from 0.2–98%, therefore at 0.2% and 10 Hz a pulse of 200 ms can be evoked reliably. For all pulses, we report the duration of the square wave TTL pulse used to trigger the LED; for each pulse there is a rise time of 51 μs and a fall time of 79 μs. For experiments in which channelrhodopsin responses were induced using an LED fiber, 0.2–3 ms light pulses were delivered through an optical fiber (PlexBright 200/230 μm Optical Patch Cable, Plexon) controlled by an LED driver (LD-1, Plexon). The fiber was placed 100–600 μm from the recording electrode and directly above the surface of the slice without actually making contact, allowing for movement of the fiber during recording. Pairs or trains of stimuli were delivered once every 30 seconds to avoid desensitization of channelrhodopsin. Series resistance was monitored throughout the experiments and cells were discarded if these values changed by more than 15% during an experiment. To isolate $GABA_A$R IPSCs,

6,7-dinitroquinoxaline-2,3-dione (DNQX; 10 μM) and strychnine (1 μM) were added to the extracellular solution to block AMPA and glycine receptors respectively. When feasible, the $GABA_AR$ blocker bicuculline (10 μM) was added at the end of experiments to confirm that all residual currents were eliminated. To induce NO-dependent LTP_{GABA}, the NO donor, S-nitroso-N-acetylpenicillamine (SNAP, 400 μM) was applied via perfused ACSF. These experiments included 3-isobutyl-1-methylxanthine (IBMX; 100 μM) in the bath for at least 10 min prior to and throughout the application of SNAP to inhibit phosphodiesterase-mediated degradation of cGMP.

Analysis:

All traces were analyzed using Clampfit software and data were graphed and analyzed using GraphPad Prism. Throughout, data are presented as mean ± SEM unless otherwise noted, and significance was defined as $p < 0.05$ **(denoted by *)**. Details of specific statistical tests used for each experiment are found in the figure legends. Inhibition of optically-evoked PSCs by pharmacological antagonists of AMPA and glycine receptors was determined by comparing the mean amplitude of PSCs for the 5 minutes immediately prior to drug application to the mean amplitude of PSCs 6–10 minutes after drug application. Magnitude of LTP was determined as mean IPSC amplitude for 10 min just before application of SNAP compared with mean IPSC amplitude from 10–20 min after SNAP application, unless otherwise noted. Paired pulse ratios and short-term plasticity during trains were determined by averaging at least eight traces. One cell was excluded from analysis of short-term plasticity during trains because it differed from the average data by >4 standard deviations. For kinetic analyses, we used an average of 10–20 traces with a single peak and a smooth decay for each cell. Rise time (time from 10–90% of peak IPSC amplitude) was measured using Clampfit software. Time constant (τ) of decay was derived by fitting a single exponential equation to the curve of the IPSC decay using Clampfit software.

Two cells were excluded from analysis of the τ_{decay} due to values that were >2 standard deviations from the mean. All n's refer to the number of cells, and each experimental group consisted of at least 4 animals.

Materials:

IBMX was obtained from Enzo Life Sciences. Bicuculline and SNAP were obtained from Tocris Biosciences. DNQX and strychnine were obtained from Sigma-Aldrich.

Results

Viral targeting of RMTg and VTA inputs

To compare functional properties of inhibitory synapses arising from the RMTg and the VTA, we utilized a virus-driven optogenetic approach to isolate synapses arising from each region. While distinguishing the RMTg from the VTA proper in a mouse has been a somewhat difficult proposition, recent studies have identified a "RMTg-like" area in the mouse midbrain that we have targeted in our experiments (Stamatakis & Stuber, 2012). To limit activation to GABAergic neurons, we used VGAT-Cre mice injected with AAV2-DIO-ChR2-eYFP in either the VTA (Figure 1A–B) or the RMTg (Figure 2A–B). For all

recordings, we examined eYFP fluorescence in slices from both the RMTg and VTA, and slices from animals exhibiting fluorescent cell bodies outside the target injection area (indicated in figure 1B and 2B) were discarded from the study. After allowing 3 weeks for viral expression, we examined the VTA histologically and electrophysiologically.

In VTA injected animals, we found eYFP-positive fibers and cell bodies in the VTA. eYFP-positive fibers were generally limited to the area immediately surrounding the injection site, suggesting that within the VTA, GABAergic neurons primarily target neighboring cells and do not appear to project widely throughout the VTA (Figure 1D–F). eYFP fluorescence was not observed in TH+ cell bodies (Figure 1G), indicating that ChR2 expression was limited to GABAergic neurons. To confirm expression of ChR2 in GABAergic neurons, we carried out current-clamp recordings in the VTA from eYFP-positive cells (i.e. VGAT-expressing GABAergic neurons). Photostimulation (0.4–4 ms, 20 Hz) reliably drove firing of action potentials in fluorescent cells (Figure 1C) followed by synaptic potentials presumably resulting from GABA release from neighboring VTA interneurons.

In RMTg-injected animals, eYFP-positive cell bodies and fibers were observed in the putative RMTg (caudal to the interpeduncular fossa, ventral to the periaqueductal gray and raphe nuclei, and interspersed with the decussating fibers of the superior cerebellar peduncle; Figure 2B, D–G). We observed a high degree of overlap between viral expression and immunostaining for the transcription factor FoxP1, a marker of the RMTg (Lahti et al., 2016; Thomas Jhou, personal communication). In contrast to the more localized innervation of VTA GABA neurons, immunohistochemical examination of VTA slices from RMTg-injected animals revealed dense, widespread, and more evenly distributed innervation of both the VTA and SNc (Figure 2H–K). Photostimulation (0.4–4 ms, 20 Hz) of eYFP-positive cells in acute slices containing the RMTg reliably induced action potentials (Figure 2C) followed by synaptic potentials presumably evoked by light-activation of neighboring RMTg neurons.

Basal synaptic properties of VTA and RMTg inputs

We examined basal properties of synaptic currents originating from RMTg and VTA afferents using patch-clamp recordings in acutely prepared coronal slices of the VTA. Our recordings were restricted to I_{h+} neurons located in the lateral portion of the VTA (unless otherwise noted), a population enriched in nucleus accumbens-projecting dopamine neurons (Lammel *et al.*, 2008, 2011, 2014; Baimel *et al.*, 2017; Edwards *et al.*, 2017). These neurons are activated by rewarding stimuli, and optogenetic activation of these dopamine neurons induces place preference (Lammel *et al.*, 2011, 2012). We voltage-clamped KCl-loaded non-fluorescent neurons in the lateral VTA and used photostimulation (0.4–4 ms) to elicit inward synaptic currents. We found reliable synaptic inputs originating from both regions, both in cells expressing a hyperpolarization induced current (I_{h+}; usually dopaminergic, Ungless and Grace, 2012), and in those without (I_h-; GABAergic, glutamatergic, and a subset of dopaminergic neurons, Lammel et al., 2008, 2012; Ungless and Grace, 2012; Baimel et al, 2017). In I_{h+} cells, we noted that synapses originating from the RMTg on average required a shorter duration of optical stimulation to elicit larger currents (Komolgorov-Smirnov test, D = 0.4971, $p = 0.007$, VTA: n = 25 cells/**23 mice**, RMTg: n = 21 cells/**21 mice**), consistent

with their reported multiple synaptic sites on dopamine cell dendrites (Jhou et al., 2009b; Figure 3A). Although less dramatic, this pattern was also seen with inputs onto I_h- neurons (Komolgorov-Smirnov test, D = 0.4329, $p = 0.04$, VTA: n = 21 cells/**21 mice**, RMTg: n = 22 cells/**22 mice**; Figure 3B). For all subsequent experiments, we recorded only from I_{h+} cells.

We next compared the kinetics of $GABA_A$R-mediated responses to photostimulation. We found that the rise time (VTA = 0.96 ± 0.08 ms, n = 10 cells; RMTg = 1.12 ± 0.09 ms, n = 13 cells; Student's t-test t = 1.328, p = 0.20; Figure 3C) and decay time constant (VTA = 4.62 ± 0.29, n = 7 cells/**6 mice**; RMTg = 5.25 ± 0.36, n = 11 cells/**9 mice**; Student's t-test t = 1.249, $p = 0.23$; Figure 3D) of evoked $GABA_A$R currents in VTA dopamine neurons did not differ between VTA and RMTg afferents. However paired-pulse ratios from VTA-originating GABAergic synapses exhibited robust paired-pulse depression, while on average RMTg synapses exhibited modest paired-pulse facilitation (VTA = 0.75 ± 0.06, n = 8 cells/**6 mice**, RMTg = 1.10 ± 0.08, n = 23 cells/**19 mice**; Mann-Whitney $U = 36$, * $p = 0.01$; Figure 3E). Given that ChR2 is a calcium-permeable cation channel, however, it is possible that alterations in release probability arise from ChR2-mediated changes in presynaptic calcium availability at the terminal (Zhang & Oertner, 2007). To control for this possibility, we compared RMTg ->VTA IPSCs in responses evoked by pairs or trains of light delivered through the objective to those evoked using a fiber optic LED We found no significant effect of stimulation type or interaction between pulse number and stimulation type, indicating that there was no effect on the short term dynamics of release (2-way ANOVA, stimulation $F_{1,8}$ = 0.6338, $p = 0.45$; pulse number $F_{9, 72} = 12.89$, * represents significant effect of pulse number, $p < 0.0001$; interaction $F_{9,72} = 0.4588$, $p = 0.90$; n = 5 cells/**4 mice** Figure 3F). We also used fiber optic light stimulation at increasing distances from a recorded cell soma and found little difference in the short-term dynamics of synaptic responses (Figure 3G). These results indicate that synaptic responses evoked with our full field light are likely to depend almost entirely on action potential generation in the axons, and are not greatly affected by direct Ca^{2+} entry through nerve terminal ChR2 channels. Taken together, these data indicate a significantly higher release probability in synapses arising from local VTA afferents.

Co-release of glutamate and glycine from VTA and RMTg afferents.

Recent studies have shown that VTA GABAergic neurons co-release glutamate in distal regions (Root *et al.*, 2014; Ntamati & Lu scher, 2016; Yoo *et al.*, 2016). To determine if this co- release also occurs at their local synapses in the VTA, we measured optically-evoked synaptic currents (PSCs) in the presence of inhibitors of AMPARs and glycine receptors (10 μM DNQX and 1 μM strychnine; Figure 4A–B). In most cells, the light-evoked synaptic current was not significantly affected by bath application of DNQX or strychnine (IPSC amplitude baseline = 205.5 ± 36.4 pA, +DNQX = 164.4 ± 35.9 pA, +strychnine = 129.0 ± 22.3 pA; one-way ANOVA corrected for sphericity, $F_{(1.091,5.455)} = 2.964$, $p = 0.14$; n = 6 cells/**6 mice**). All residual currents after DNQX and strychnine administration were blocked by the $GABA_A$R antagonist bicuculline (30 μM) (4B). These data suggest that there is little or no co-release of glutamate or glycine at local synapses between VTA GABAergic neurons and dopamine neurons.

PSCs evoked by photostimulation of RMTg afferents were also not inhibited by DNQX, and in many cells actually increased in amplitude, indicating that glutamate is not co-released from these axons (4C-D). Application of strychnine after addition of DNQX, however, significantly decreased the PSC amplitude, suggesting that the RMTg terminals can co-release glycine in the VTA. (IPSC amplitude baseline = 350.4 ± 79.9 pA, +DNQX = 410.7 ± 99.3 pA, +strychnine = 329.2 ± 89.4 pA; one-way ANOVA corrected for sphericity, $F_{(1.675,10.05)} = 7.337$, $p = 0.01$; n = 7 cells/**7 mice)**. To confirm that RMTg inputs can indeed co-release glycine, we tested a separate set of cells to which we applied strychnine alone. Again IPSC amplitude was decreased (IPSC amplitude baseline = 278.3 ± 59.9 pA, strychnine = 201.5 ± 56.3 pA, paired t-test, $p = 0.05$, n = 6 cells/**5 mice**). Therefore, local VTA inhibitory synapses onto VTA dopamine neurons primarily release GABA, with little to no co-release of glutamate or glycine, while RMTg synapses onto dopamine neurons co-release GABA and glycine.

Short-term plasticity of VTA and RMTg inputs

Short-term facilitation and depression of synapses can powerfully shape the information carried by repetitive trains of action potentials. To investigate this, we next compared short-term plasticity of GABAergic synapses made by RMTg and VTA afferents during trains of different frequencies. During voltage clamp recordings from VTA dopamine neurons, we stimulated trains of ten light-evoked $GABA_AR$ currents at 5 or 20 Hz (Figure 5). In VTA-originating synapses, both 5 and 20 Hz stimulation depressed IPSC amplitude over the course of the train, however; the depression was significantly larger at the 20 Hz frequency (two-way repeated measure ANOVA: stimulation frequency $F_{(1,11)} = 6.268$, $p = 0.03$, interaction $F_{(9,99)} = 1.535$, p = 0.15; n = 8 cells/6 **mice** (20 Hz) and 5 cells/5 **mice** (5 Hz). Figure 5A–B). In contrast, RMTg-originating synapses exhibited moderate depression that did not significantly differ between 5 Hz and 20 Hz (Two-way repeated measure ANOVA: stimulation frequency $F_{(1,27)} = 0.2$, $p = 0.66$, interaction $F_{(9,243)} = 0.8703$, p = 0.55; n = 23 cells/19 **mice** (20 Hz) and 6 cells/6 **mice** (5 Hz). Thus, VTA- but not RMTg-originating synapses exhibit short-term depression with a magnitude that is dependent on the frequency of stimulation.

Long-term plasticity of VTA and RMTg inputs

Our lab previously characterized long-term potentiation at $GABA_AR$ synapses on VTA dopamine neurons (LTP_{GABA}) using electrical stimulation within the VTA of presumably mixed GABAergic afferents (Nugent *et al*, 2007). LTP_{GABA} is a heterosynaptic form of plasticity, induced when Ca^{2+} entry through postsynaptic NMDA receptors causes activation of nitric oxide synthase and production of nitric oxide (NO). NO, acting as a retrograde messenger, triggers a persistent increase in GABA release by activating cGMP/PKG signaling in the presynaptic terminal. Accordingly, exogenous application of the NO donor SNAP can be used to induce LTP_{GABA} (Nugent *et al.*, 2007, 2009). Our recent work has shown that LTP_{GABA} is blocked after a single in vivo exposure to either drugs of abuse or stress (Niehaus et al., 2010), and that this loss is correlated with stress-induced reinstatement of drug seeking (Graziane *et al.*, 2013; Polter *et al.*, 2014, 2017). To examine the differential involvement of RMTg and VTA inputs, we next tested whether each input was capable of expressing NO-dependent LTP_{GABA}.

At $GABA_AR$ synapses arising from local VTA GABAergic neurons, we found that bath application of SNAP potentiated the optically evoked IPSCs (Figure 6A,C,D). While potentiation was observed in the majority of these experiments, we noted that on average SNAP-induced potentiation was of smaller magnitude than that typically seen with less selective electrical stimulation. Although our prior studies indicated that NO-dependent LTP_{GABA} is expressed in the presynaptic terminal (Nugent *et al.*, 2007, 2009), in the VTA→VTA cells that potentiated with SNAP, the paired-pulse ratios were not significantly decreased as expected with a presynaptic locus of potentiation (baseline = 0.67 ± 0.04, post-SNAP = 0.72 ± 0.7, paired t-test, $p = 0.49$; n = 6 cells/6 **mice**, Figure 6E). In contrast to the potentiation seen at VTA-originating GABAergic synapses, at $GABA_AR$ synapses from the RMTg on VTA neurons, bath application of SNAP did not elicit potentiation (normalized IPSC amplitude, VTA = 129 ± 9% baseline, n = 11 cells/11 **mice**; RMTg = 89 ± 9% baseline, n = 8 cells/8 **mice**; Student's t-test, t = 3.089, represents significant difference between RMTg and VTA, $p = 0.007$; Figure 6B–D). In fact, in roughly half of the cells SNAP modestly depressed synaptic transmission. Together our results show that in addition to differences in short-term plasticity, RMTg and local VTA synapses also exhibit distinct long-term plasticity in response to NO.

Discussion

Afferent distribution and basal function

The RMTg and local VTA GABA neurons are two significant sources of inhibitory input onto VTA dopaminergic neurons. Although the existence of the RMTg as a separate entity from the VTA was once controversial, recent studies indicate that the RMTg is a distinct functional and anatomical region in both rats and mice (Jhou *et al.*, 2009a; Bourdy & Barrot, 2012; Stamatakis & Stuber, 2012; Bourdy *et al.*, 2014). In this study, we used viral-mediated optogenetics to characterize synaptic function and plasticity of inhibitory synapses from each region onto VTA dopamine neurons.

We observed a striking difference in the distribution of axons arising from the two regions, with VTA-originating axons appearing much more limited in spread within the VTA. In contrast, the widespread and uniform distribution of RMTg axons suggests that these inputs may coordinate activity across the VTA, and even to the SNc as well. This is consistent with a proposed role for the RMTg as a "funnel" integrating converging inputs from multiple aversion- related brain areas to inhibit activity of VTA and SNc dopaminergic neurons (Jhou *et al.*, 2009b; Kaufling *et al.*, 2009; Bourdy & Barrot, 2012). The more limited and local distribution of VTA GABAergic axons (Ferreira *et al.*, 2008; Omelchenko & Sesack, 2009) may instead allow distinct subsets of GABAergic neurons to segregate control of differentially-projecting dopamine neurons, which are topographically organized into functionally distinct groups (Lammel *et al.*, 2014). Alternatively, VTA GABAergic neurons have been reported to be electrically coupled via gap junctions (Stobbs *et al.*, 2004; Allison *et al.*, 2006), which could synchronize inhibitory signals originating in these neurons across longer ranges within the VTA without requiring axonal connectivity. We also noted that a given photostimulus duration evoked on average a larger IPSC in afferents from RMTg compared to those from VTA. This observation may result from a denser innervation by

RMTg fibers, but may also reflect other experimental variables such as relative uptake or expression of virus.

Co-release of GABA and glycine

Our results with selective receptor antagonists indicate that RMTg-originating GABAergic afferent synapses nearly uniformly co-release glycine, a fast inhibitory neurotransmitter prevalent in the hindbrain and spinal cord. Our experiments cannot distinguish true co-release from single nerve terminals (as reported for glycine and GABA release in spinal cord and brainstem synapses; Jonas *et al.*, 1998; Russier *et al.*, 2002; Rahman *et al.*, 2013; Moore & Trussell, 2017) from separate glycinergic and GABAergic synapses within the same population of GABAergic afferents onto a given dopamine neuron. While the functional consequence of glycine co-release remains unknown, in the spinal cord and brainstem co-released glycine and GABA frequently play distinct roles in fine tuning neuronal transmission through the differing kinetics of their receptors or transporters (Russier *et al.*, 2002; Rahman *et al.*, 2013), and can exhibit independent synaptic plasticity (Chirila *et al.*, 2014). In contrast, glycinergic and GABAergic responses follow similar time courses in the auditory midbrain (Moore & Trussell, 2017), suggesting that the two transmitters may in some cases be functionally interchangeable.

Intriguingly, PSCs evoked from RMTg afferents frequently *increased* in amplitude following application of DNQX. One potential explanation for this phenomenon is that concurrently active AMPA receptors shunt inhibitory current from GABA and glycine receptors and that blocking AMPA receptors removes the shunt. The presence of this effect at most RMTg afferent synapses but not at VTA afferent synapses suggests that GABAergic/glycinergic synapses from the RMTg may be located more proximal to concurrently active excitatory synapses than synapses from local VTA GABA neurons. Alternatively, it is possible that RMTg nerve terminals express presynaptic kainate or AMPARs, which can inhibit presynaptic GABAergic nerve terminals (Lee *et al.*, 2002; Rusakov, 2005; Bonfardin *et al.*, 2010; Daw *et al.*, 2010); bath application of DNQX could relieve a tonic inhibition of GABA release from RMTg nerve terminals resulting from ambient levels of glutamate (Sah *et al.*, 1989) producing the observed increase in IPSC amplitude.

At most synapses arising from local VTA neurons, optically-evoked PSCs were insensitive to both DNQX and strychnine, however, it should be noted that a few (~25%) of these synaptic inputs were depressed by DNQX, and thus there may be a subset of local GABAergic neurons that co-release glutamate. This is consistent with recent reports that VTA GABA neurons projecting to habenula, dentate gyrus, or ventral pallidum co-release glutamate (Root *et al.*, 2014; Ntamati & Lu scher, 2016; Yoo *et al.*, 2016). Whether the divergence in the ability of local VTA GABA neurons to co-release glutamate arises from distinct subtypes of VTA GABAergic neurons remains to be determined. However, this observation also suggests that blockade or loss of $GABA_A$Rs at synapses from VTA GABAergic neurons could unmask a previously blunted excitatory input onto target cells. In contrast, the co-release of glycine from RMTg afferents would instead only enhance the inhibitory strength of these afferents.

Differing short- and long-term plasticity at RMTg and VTA afferent synapses

The two inputs differ in their paired-pulse ratio, with VTA synapses exhibiting paired-pulse depression, suggesting a higher initial release probability. Over longer trains of action potentials, synapses originating from the RMTg exhibit fairly consistent GABA release regardless of stimulation frequency (5 or 20 Hz). RMTg neurons typically fire at approximately 15–20 Hz *in vivo* (Jhou *et al.*, 2009a; Jalabert *et al.*, 2011; Lecca *et al.*, 2011), but in many RMTg neurons, the firing rate drops precipitously upon presentation of a reward or reward-related cue (Jhou *et al.*, 2009a). Therefore, repeated action potentials from RMTg to VTA cells are expected to be equally effective at inhibiting VTA neurons across a range of frequencies, even if those frequencies represent different information. In contrast, VTA GABA cell synapses exhibit synaptic depression that increases at higher frequency. Reported values of the natural firing rate of VTA GABA neurons are highly variable, ranging from 2–20 Hz (Steffensen *et al.*, 1998; Gallegos *et al.*, 1999; Cohen *et al.*, 2012; Tan *et al.*, 2012), with rapid and robust increases in firing rate induced by aversive stimuli (Cohen *et al.*, 2012; Tan *et al.*, 2012). Although aversive and rewarding stimuli have broadly similar effects on firing rate in both VTA and RMTg GABA neurons, increased frequency in the VTA→VTA synapses is expected to result in decreasing GABA release, while inhibitory inputs from RMTg are expected to remain more consistent across a train. Viral expression of channelrhodopsin can in some cases artificially increase release probability (Zhang & Oertner, 2007; Jackman *et al.*, 2014), however, suggesting caution is warranted when interpreting these results. Our control experiments indicate that the GABA release we measured during trains and paired pulses results from action potentials invading the presynaptic terminals rather than from direct Ca^{2+} entry through nerve terminal ChR2 channels. These data provide confidence that our light-evoked responses mimic normal action potential- dependent release properties.

We also show that synaptic inputs from VTA GABA neurons, but not from RMTg GABA neurons, exhibit nitric-oxide dependent LTP_{GABA}. It is not surprising that VTA GABA neurons would exhibit this form of plasticity, as our earlier studies of LTP_{GABA} utilized electrical stimulation in the VTA itself and most reliably would have activated these inputs. However, there were notable differences between optically- and electrically-evoked LTP_{GABA}. While our previous studies suggested a presynaptic site of NO action (Nugent *et al.*, 2007, 2009), as indicated by a decrease in the paired pulse ratio, we did not observe this decrease at all potentiated VTA GABA synapses in the current study. Furthermore, although synapses arising from VTA GABA neurons did exhibit reliable LTP, it was of smaller magnitude than in our previous studies utilizing electrical stimulation (Nugent *et al.*, 2007, 2009; Niehaus *et al.*, 2010; Graziane *et al.*, 2013; Polter *et al.*, 2014, 2017). Notably, our data are consistent with a recent report using a similar approach, both with respect to the circuit specificity and magnitude of LTP_{GABA} (Simmons *et al.*, 2017). These authors also reported that optically activated nucleus accumbens GABAergic inputs exhibit LTP_{GABA} as well (Simmons *et al.*, 2017). The differences between optically- and electrically-evoked LTP_{GABA} could alternatively result from differences in the species and/or age of the animals. It is further possible that additional inputs such as the ventral pallidum (Hjelmstad *et al.*, 2013), periaqueductal grey (Omelchenko & Sesack, 2010) or dorsal raphe (Geisler & Zahm, 2005) contribute to electrically-evoked IPSCs, and thus to the plasticity recorded in prior

studies. The mechanism by which NO-cGMP potentiates the release of GABA from these synapses is unknown, however, and it is also possible that presynaptic ChR2 expression in VTA GABAergic afferents interacts with the induction of LTP_{GABA}. Finally, given the stress-sensitivity of LTP_{GABA} (Niehaus *et al.*, 2010), it is possible that the stress of stereotaxic surgery and/or single-housing after surgery partially inhibits LTP_{GABA}.

The inability of inhibitory inputs from RMTg→VTA dopamine neurons to exhibit synaptic plasticity suggests that they are differentially regulated. We reported previously that electrically-evoked $GABA_BR$ synaptic responses on VTA dopamine neurons (likely arising from the nucleus accumbens, Edwards *et al.*, 2017) do not potentiate in response to nitric oxide (Nugent *et al.*, 2009), similarly indicating that at least some GABAergic terminals in the VTA do not have the necessary signaling machinery for LTP_{GABA}. However, it was shown previously that the lack of potentiation in RMTg-originating inputs was not correlated with a change in presynaptic guanylate cyclase in RMTg neurons (Simmons et al., 2017), suggesting that GC/cGMP signaling is normal in those terminals. In that study, light activation of ChR2 afferents from each region was used to evoke IPSCs, but LTP was triggered using electrical high-frequency stimulation, rather than a nitric oxide donor, as in our experiments. The similarity in our results support the idea that the two methods of evoking LTP produce the same form of synaptic plasticity.

Inhibitory synapses in the heterogeneous VTA circuit

Neuromodulatory signals may also be localized only to specific synaptic inputs. Our previous work showed that the block of LTP_{GABA} requires activation of kappa opioid receptors (Graziane et al., 2013; Polter et al., 2014; Polter et al., 2017). While not tested as yet, expression of LTP_{GABA} at VTA- but not RMTg-originating $GABA_AR$ synapses raises the possibility that κOR activation has selective effects on plasticity at local inhibitory synapses arising from VTA GABA neurons. This input-selectivity is likely true for many neuromodulators, as serotonin, adenosine, and dopamine receptors also selectively modulate synapses arising from distinct brain regions (Johnson *et al.*, 1992; Cameron & Williams, 1993; Bonci & Williams, 1997; Shoji *et al.*, 1999; Matsui *et al.*, 2014; Edwards *et al.*, 2017).

Given that both the RMTg and VTA GABAergic neurons play significant roles in aversion and in “anti-reward” signaling (Bourdy & Barrot, 2012; Creed *et al.*, 2014), it is not surprising that that they would form inhibitory connections with reward-encoding, accumbens-projecting dopamine neurons, those we are most likely to have included in our recordings. While it remains unknown whether both sets of GABAergic neurons also form synaptic connections with other dopamine neuron subsets, it is likely that they do, given that we frequently observed photostimulated IPSCs on I_h- cells. Future investigations of the circuit connectivity patterns among these neurons will be particularly valuable.

Acknowledgements

The authors thank Dr. Scott Cruickshank, Dr. Michelle Fogerson, and Rudy Chen for assistance in setting up viral injections, Dr. Geoff Williams and the Leduc Bioimaging Facility for assistance with microscopy, and Dr. Thomas Jhou for the suggestion of using FoxP1 staining as a marker for the RMTg. This research was supported by: R01DA011289 (JAK), K99MH106757 (AMP), a NARSAD Young Investigator Award from the Brain and Behavior Research Foundation (AMP), F32DA043924 (KB) and an undergraduate teaching and research award from Brown University (ACT).

References

Allison DW, Ohran AJ, Stobbs SH, Mameli M, Valenzuela CF, Sudweeks SN, Ray AP, Henriksen SJ, & Steffensen SC (2006) Connexin-36 gap junctions mediate electrical coupling between ventral tegmental area GABA neurons. Synapse, 60, 20–31. [PubMed: 16575850]

Authement ME, Kodangattil JN, Gouty S, Rusnak M, Symes AJ, Cox BM, & Nugent FS (2015) Histone Deacetylase Inhibition Rescues Maternal Deprivation-Induced GABAergic Metaplasticity through Restoration of AKAP Signaling. Neuron, 86, 1240–1252. [PubMed: 26050042]

Baimel C & Borgland SL (2015) Orexin Signaling in the VTA Gates Morphine-Induced Synaptic Plasticity. J. Neurosci, 35, 7295–7303. [PubMed: 25948277]

Baimel C, Lau BK, Qiao M, & Borgland SL (2017) Projection-Target-Defined Effects of Orexin and Dynorphin on VTA Dopamine Neurons. Cell Rep, 18, 1346–1355. [PubMed: 28178514]

Bocklisch C, Pascoli V, Wong JCY, House DRC, Yvon C, de Roo M, Tan KR, & Luscher C (2013) Cocaine Disinhibits Dopamine Neurons by Potentiation of GABA Transmission in the Ventral Tegmental Area. Science, 341, 1521–1525. [PubMed: 24072923]

Bonci A & Williams JT (1997) Increased probability of GABA release during withdrawal from morphine. J Neurosci, 17, 796–803. [PubMed: 8987801]

Bonfardin VDJ, Fossat P, Theodosis DT, & Oliet SHR (2010) Glia-Dependent Switch of Kainate Receptor Presynaptic Action. J. Neurosci, 30, 985–995. [PubMed: 20089907]

Bourdy R & Barrot M (2012) A new control center for dopaminergic systems: Pulling the VTA by the tail. Trends Neurosci, 35, 681–690. [PubMed: 22824232]

Bourdy R, Sánchez-Catalán M-J, Kaufling J, Balcita-Pedicino JJ, Freund-Mercier M-J, Veinante P, Sesack SR, Georges F, & Barrot M (2014) Control of the Nigrostriatal Dopamine Neuron Activity and Motor Function by the Tail of the Ventral Tegmental Area. Neuropsychopharmacology, 39, 2788–2798. [PubMed: 24896615]

Cameron DL & Williams JT (1993) Dopamine D1 receptors facilitate transmitter release. Nature, 366, 344–347. [PubMed: 8247128]

Chergui K, Charléty PJ, Akaoka H, Saunier CF, Brunet J-L, Buda M, Svensson TH, & Chouvet G (1993) Tonic Activation of NMDA Receptors Causes Spontaneous Burst Discharge of Rat Midbrain Dopamine Neurons *In Vivo*. Eur. J. Neurosci, 5, 137–144. [PubMed: 8261095]

Chirila AM, Brown TE, Bishop RA, Bellono NW, Pucci FG, & Kauer JA (2014) Long-term potentiation of glycinergic synapses triggered by interleukin 1β. Proc. Natl. Acad. Sci. U. S. A, 111, 8263–8268. [PubMed: 24830427]

Cohen JY, Haesler S, Vong L, Lowell BB, & Uchida N (2012) Neuron-type-specific signals for reward and punishment in the ventral tegmental area. Nature, 482, 85–88. [PubMed: 22258508]

Creed MC, Ntamati NR, & Tan KR (2014) VTA GABA neurons modulate specific learning behaviors through the control of dopamine and cholinergic systems. Front. Behav. Neurosci, 8, 8. [PubMed: 24478655]

Daw MI, Pelkey KA, Chittajallu R, & McBain CJ (2010) Presynaptic Kainate Receptor Activation Preserves Asynchronous GABA Release Despite the Reduction in Synchronous Release from Hippocampal Cholecystokinin Interneurons. J. Neurosci, 30, 11202–11209. [PubMed: 20720128]

Edwards NJ, Tejeda HA, Pignatelli M, Zhang S, McDevitt RA, Wu J, Bass CE, Bettler B, Morales M, & Bonci A (2017) Circuit specificity in the inhibitory architecture of the VTA regulates cocaine-induced behavior. Nat. Neurosci, 20, 438–448. [PubMed: 28114294]

Ferreira JGP, Del-Fava F, Hasue RH, & Shammah-Lagnado SJ (2008) Organization of ventral tegmental area projections to the ventral tegmental area–nigral complex in the rat. euroscience, 153, 196–213.

Gallegos RA, Lee RS, Criado JR, Henriksen SJ, & Steffensen SC (1999) Adaptive responses of gamma-aminobutyric acid neurons in the ventral tegmental area to chronic ethanol. J. Pharmacol. Exp. Ther, 291, 1045–1053. [PubMed: 10565823]

Geisler S & Zahm DS (2005) Afferents of the ventral tegmental area in the rat-anatomical substratum for integrative functions. J. Comp. Neurol, 490, 270–294. [PubMed: 16082674]

Graziane NM, Polter AM, Briand LA, Pierce RC, & Kauer JA (2013) Kappa opioid receptors regulate stress-induced cocaine seeking and synaptic plasticity. Neuron, 77, 942–954. [PubMed: 23473323]

Guan Y & Ye J-H (2010) Ethanol blocks long-term potentiation of GABAergic synapses in the ventral tegmental area involving mu-opioid receptors. Neuropsychopharmacology, 35, 1841–1849. [PubMed: 20393452]

Haber SN, Groenewegen HJ, Grove EA, & Nauta WJH (1985) Efferent connections of the ventral pallidum: Evidence of a dual striato pallidofugal pathway. J. Comp. Neurol, 235, 322–335. [PubMed: 3998213]

Hjelmstad GO, Xia Y, Margolis EB, & Fields HL (2013) Opioid modulation of ventral pallidal afferents to ventral tegmental area neurons. J. Neurosci, 33, 6454–6459. [PubMed: 23575843]

Holly EN & Miczek KA (2016) Ventral tegmental area dopamine revisited: Effects of acute and repeated stress. Psychopharmacology (Berl), 233, 163–186. [PubMed: 26676983]

Jackman SL, Beneduce BM, Drew IR, & Regehr WG (2014) Achieving High-Frequency Optical Control of Synaptic Transmission. J. Neurosci, 34, 7704–7714. [PubMed: 24872574]

Jalabert M, Bourdy R, Courtin J, Veinante P, Manzoni OJ, Barrot M, & Georges F (2011) Neuronal circuits underlying acute morphine action on dopamine neurons. Proc. Natl. Acad. Sci. U. S. A, 108, 16446–16450. [PubMed: 21930931]

Jennings JH, Sparta DR, Stamatakis AM, Ung RL, Pleil KE, Kash TL, & Stuber GD (2013) Distinct extended amygdala circuits for divergent motivational states. Nature, 496, 224–228. [PubMed: 23515155]

Jhou TC, Fields HL, Baxter MG, Saper CB, & Holland PC (2009a) The Rostromedial Tegmental Nucleus (RMTg), a GABAergic Afferent to Midbrain Dopamine Neurons, Encodes Aversive Stimuli and Inhibits Motor Responses. Neuron, 61, 786–800. [PubMed: 19285474]

Jhou TC, Geisler S, Marinelli M, Degarmo BA, & Zahm DS (2009b) The mesopontine rostromedial tegmental nucleus: A structure targeted by the lateral habenula that projects to the ventral tegmental area of Tsai and substantia nigra compacta. J. Comp. Neurol, 513, 566–596. [PubMed: 19235216]

Johnson SW, Mercuri NB, & North RA (1992) 5-hydroxytryptamine1B receptors block the GABAB synaptic potential in rat dopamine neurons. J. Neurosci, 12, 2000–2006. [PubMed: 1578282]

Johnson SW & North RA (1992) Opioids excite dopamine neurons by hyperpolarization of local interneurons. J. Neurosci, 12, 483–488. [PubMed: 1346804]

Jonas P, Bischofberger J, & Sandkühler J (1998) Corelease of two fast neurotransmitters at a central synapse. Science, 281, 419–424. [PubMed: 9665886]

Kaufling J & Aston-Jones G (2015) Persistent Adaptations in Afferents to Ventral Tegmental Dopamine Neurons after Opiate Withdrawal. J. Neurosci, 35, 10290–10303. [PubMed: 26180204]

Kaufling J, Veinante P, Pawlowski SA, Freund-Mercier M-J, & Barrot M (2009) Afferents to the GABAergic tail of the ventral tegmental area in the rat. J. Comp. Neurol, 513, 597–621. [PubMed: 19235223]

Lahti L, Haugas M, Tikker L, Airavaara M, Voutilainen MH, Anttila J, Kumar S, Inkinen C, Salminen M, & Partanen J (2016) Differentiation and molecular heterogeneity of inhibitory and excitatory neurons associated with midbrain dopaminergic nuclei. Development, 143, 516–529. [PubMed: 26718003]

Lammel S, Hetzel A, H?ckel O, Jones I, Liss B, & Roeper J (2008) Unique Properties of Mesoprefrontal Neurons within a Dual Mesocorticolimbic Dopamine System. Neuron, 57, 760–773. [PubMed: 18341995]

Lammel S, Ion DIDI, Roeper J, & Malenka RRCC (2011) Projection-Specific Modulation of Dopamine Neuron Synapses by Aversive and Rewarding Stimuli. Neuron, 70, 855–862. [PubMed: 21658580]

Lammel S, Lim BK, & Malenka RC (2014) Reward and aversion in a heterogeneous midbrain dopamine system. Neuropharmacology, 76, 351–359. [PubMed: 23578393]

Lammel S, Lim BK, Ran C, Huang KW, Betley MJ, Tye KM, Deisseroth K, & Malenka RC (2012) Input-specific control of reward and aversion in the ventral tegmental area. Nature, 491, 212–217. [PubMed: 23064228]

Lecca S, Melis M, Luchicchi A, Ennas MG, Castelli MP, Muntoni AL, & Pistis M (2011) Effects of Drugs of Abuse on Putative Rostromedial Tegmental Neurons, Inhibitory Afferents to Midbrain Dopamine Cells. Neuropsychopharmacology, 36, 589–602. [PubMed: 21048703]

Lecca S, Melis M, Luchicchi A, Muntoni AL, & Pistis M (2012) Inhibitory Inputs from Rostromedial Tegmental Neurons Regulate Spontaneous Activity of Midbrain Dopamine Cells and Their Responses to Drugs of Abuse. Neuropsychopharmacology, 37, 1164–1176. [PubMed: 22169942]

Lee CJ, Bardoni R, Tong C-K, Engelman HS, Joseph DJ, Magherini PC, & MacDermott AB (2002) Functional Expression of AMPA Receptors on Central Terminals of Rat Dorsal Root Ganglion Neurons and Presynaptic Inhibition of Glutamate Release. Neuron, 35, 135–146. [PubMed: 12123614]

Liu Q, Pu L, & Poo M (2005) Repeated cocaine exposure in vivo facilitates LTP induction in midbrain dopamine neurons. Nature, 437, 1027–1031. [PubMed: 16222299]

Matsui A, Jarvie BC, Robinson BG, Hentges ST, & Williams JT (2014) Separate GABA afferents to dopamine neurons mediate acute action of opioids, development of tolerance, and expression of withdrawal. Neuron, 82, 1346–1356. [PubMed: 24857021]

Matsui A & Williams JT (2011) Opioid-sensitive GABA inputs from rostromedial tegmental nucleus synapse onto midbrain dopamine neurons. J. Neurosci, 31, 17729–17735. [PubMed: 22131433]

Melis M, Camarini R, Ungless MA, & Bonci A (2002) Long-lasting potentiation of GABAergic synapses in dopamine neurons after a single in vivo ethanol exposure. J Neurosci, 22, 2074–2082. [PubMed: 11896147]

Mereu G, Lilliu V, Casula A, Vargiu P., Diana M, Musa A, & Gessa G. (1997) Spontaneous bursting activity of dopaminergic neurons in midbrain slices from immature rats: role of N-methyl-d-aspartate receptors. Neuroscience, 77, 1029–1036. [PubMed: 9130784]

Moore LA & Trussell LO (2017) Co-release of inhibitory neurotransmitters in the mouse auditory midbrain Co-release in the mouse auditory midbrain. J. Neurosci, 1125–17.

Morales M & Margolis EB (2017) Ventral tegmental area: cellular heterogeneity, connectivity and behaviour. Nat Rev Neurosci, 18, 73–85. [PubMed: 28053327]

Nair-Roberts RG, Chatelain-Badie SD, Benson E, White-Cooper H, Bolam JP, & Ungless MA (2008) Stereological estimates of dopaminergic, GABAergic and glutamatergic neurons in the ventral tegmental area, substantia nigra and retrorubral field in the rat. Neuroscience, 152, 1024–1031. [PubMed: 18355970]

Niehaus JL, Cruz-Bermúdez ND, & Kauer JA (2009) Plasticity of Addiction: A Mesolimbic Dopamine Short-Circuit? Am. J. Addict, 18, 259–271. [PubMed: 19444729]

Niehaus JL, Murali M, & Kauer JA (2010) Drugs of abuse and stress impair LTP at inhibitory synapses in the ventral tegmental area. Eur. J. Neurosci, 32, 108–117. [PubMed: 20608969]

Ntamati NR & Lu scher C (2016) VTA Projection Neurons Releasing GABA and Glutamate in the Dentate Gyrus. eNeuro, 3.

Nugent FS, Niehaus JL, & Kauer JA (2009) PKG and PKA Signaling in LTP at GABAergic Synapses. Neuropsychopharmacology, 345, 1829–1842.

Nugent FS, Penick EC, & Kauer J. a (2007) Opioids block long-term potentiation of inhibitory synapses. Nature, 446, 1086–1090. [PubMed: 17460674]

Omelchenko N & Sesack SR (2009) Ultrastructural analysis of local collaterals of rat ventral tegmental area neurons: GABA phenotype and synapses onto dopamine and GABA cells. Synapse, 63, 895–906. [PubMed: 19582784]

Omelchenko N & Sesack SR (2010) Periaqueductal gray afferents synapse onto dopamine and GABA neurons in the rat ventral tegmental area. J. Neurosci. Res, 88, 981–991. [PubMed: 19885830]

Ostroumov A, Thomas AM, Kimmey BA, Karsch JS, Doyon WM, & Dani JA (2016) Stress Increases Ethanol Self-Administration via a Shift toward Excitatory GABA Signaling in the Ventral Tegmental Area. Neuron, 92, 493–504. [PubMed: 27720487]

Paladini CA, Celada P, & Tepper JM (1999a) Striatal, pallidal, and pars reticulata evoked inhibition of nigrostriatal dopaminergic neurons is mediated by GABA(A) receptors in vivo. Neuroscience, 89, 799–812. [PubMed: 10199614]

Paladini CA, Iribe Y, & Tepper JM (1999b) GABA(A) receptor stimulation blocks NMDA-induced bursting of dopaminergic neurons in vitro by decreasing input resistance. Brain Res, 832, 145–151. [PubMed: 10375660]

Paxinos G & Franklin K (2012) Paxinos and Franklin's the Mouse Brain in Stereotaxic Coordinates, Amsterdam, Academic Press.

Polter AM, Barcomb K, Chen RW, Dingess PM, Graziane NM, Brown TE, & Kauer JA (2017) Constitutive activation of kappa opioid receptors at ventral tegmental area inhibitory synapses following acute stress. Elife, 6, 358–361.

Polter AM, Bishop RA, Briand LA, Graziane NM, Pierce RC, & Kauer JA (2014) Poststress block of kappa opioid receptors rescues long-term potentiation of inhibitory synapses and prevents reinstatement of cocaine seeking. Biol. Psychiatry, 76, 785–793. [PubMed: 24957331]

Rahman J, Latal AT, Besser S, Hirrlinger J, & Hülsmann S (2013) Mixed miniature postsynaptic currents resulting from co-release of glycine and GABA recorded from glycinergic neurons in the neonatal respiratory network. Eur. J. Neurosci, 37, 1229–1241. [PubMed: 23347272]

Root DH, Mejias-Aponte CA, Zhang S, Wang H-L, Hoffman AF, Lupica CR, & Morales M (2014) Single rodent mesohabenular axons release glutamate and GABA. Nat. Neurosci, 17, 1543–1551. [PubMed: 25242304]

Rusakov DA (2005) Modulation of Presynaptic Ca2+ Entry by AMPA Receptors at Individual GABAergic Synapses in the Cerebellum. J. Neurosci, 25, 4930–4940. [PubMed: 15901774]

Russier M, Kopysova IL, Ankri N, Ferrand N, & Debanne D (2002) GABA and glycine co-release optimizes functional inhibition in rat brainstem motoneurons in vitro. J. Physiol, 541, 123–137. [PubMed: 12015425]

Sah P, Hestrin S, & Nicoll R (1989) Tonic activation of NMDA receptors by ambient glutamate enhances excitability of neurons. Science, 246, 815–818. [PubMed: 2573153]

Sharpe MJ, Marchant NJ, Whitaker LR, Richie CT, Zhang YJ, Campbell EJ, Koivula PP, Necarsulmer JC, Mejias-Aponte C, Morales M, Pickel J, Smith JC, Niv Y, Shaham Y, Harvey BK, & Schoenbaum G (2017) Lateral Hypothalamic GABAergic Neurons Encode Reward Predictions that Are Relayed to the Ventral Tegmental Area to Regulate Learning. Curr. Biol, 27, 2089–2100.e5. [PubMed: 28690111]

Shoji Y, Delfs J, & Williams JT (1999) Presynaptic Inhibition of GABAB-Mediated Synaptic Potentials in the Ventral Tegmental Area during Morphine Withdrawal. J. Neurosci, 19, 2347–2355. [PubMed: 10066284]

Simmons DV, Petko AK, & Paladini CA (2017) Differential Expression of Long Term Potentiation among Identified Inhibitory Inputs to Dopamine Neurons. J. Neurophysiol, 4, 1998–2008.

Stamatakis AM & Stuber GD (2012) Activation of lateral habenula inputs to the ventral midbrain promotes behavioral avoidance. Nat. Neurosci, 15, 1105–1107. [PubMed: 22729176]

Steffensen SC, Svingos AL, Pickel VM, & Henriksen SJ (1998) Electrophysiological characterization of GABAergic neurons in the ventral tegmental area. J. Neurosci, 18, 8003–8015. [PubMed: 9742167]

Stobbs SH, Ohran AJ, Lassen MB, Allison DW, Brown JE, & Steffensen SC (2004) Ethanol Suppression of Ventral Tegmental Area GABA Neuron Electrical Transmission Involves N-Methyl-D-aspartate Receptors. J. Pharmacol. Exp. Ther, 311, 282–289. [PubMed: 15169831]

Suaud-Chagny MF, Chergui K, Chouvet G, & Gonon F (1992) Relationship between dopamine release in the rat nucleus accumbens and the discharge activity of dopaminergic neurons during local in vivo application of amino acids in the ventral tegmental area. Neuroscience, 49, 63–72. [PubMed: 1357587]

Tan KR, Yvon C, Turiault M, Mirzabekov JJ, Doehner J, Labouèbe G, Tye KM, & Lüscher C (2012) GABA Neurons of the VTA Drive Conditioned Place Aversion. Neuron, 73, 1173–1183. [PubMed: 22445344]

Taylor SR, Badurek S, Dileone RJ, Nashmi R, Minichiello L, & Picciotto MR (2014) GABAergic and glutamatergic efferents of the mouse ventral tegmental area. J. Comp. Neurol, 522, 3308–3334. [PubMed: 24715505]

Ting J, Daigle T, Chen Q, & Feng G (2014) Patch-Clamp Methods and Protocols. Methods Mol. Biol, 1183, 1–21. [PubMed: 25023299]

Ungless MA & Grace AA (2012) Are you or aren't you? Challenges associated with physiologically identifying dopamine neurons. Trends Neurosci, 35, 422–430. [PubMed: 22459161]

Van Zessen R, Phillips JL, Budygin EA, & Stuber GD (2012) Activation of VTA GABA Neurons Disrupts Reward Consumption. Neuron, 73, 1184–1194. [PubMed: 22445345]

Vong L, Ye C, Yang Z, Choi B, Chua S, & Lowell BB (2011) Leptin Action on GABAergic Neurons Prevents Obesity and Reduces Inhibitory Tone to POMC Neurons. Neuron, 71, 142–154. [PubMed: 21745644]

Xia Y, Driscoll JR, Wilbrecht L, Margolis EB, Fields HL, & Hjelmstad GO (2011) Nucleus Accumbens Medium Spiny Neurons Target Non-Dopaminergic Neurons in the Ventral Tegmental Area. J. Neurosci, 31, 7811–7816. [PubMed: 21613494]

Yoo JH, Zell V, Gutierrez-Reed N, Wu J, Ressler R, Shenasa MA, Johnson AB, Fife KH, Faget L, & Hnasko TS (2016) Ventral tegmental area glutamate neurons co- release GABA and promote positive reinforcement. Nat. Commun, 7, 13697. [PubMed: 27976722]

Zhang Y-P & Oertner TG (2007) Optical induction of synaptic plasticity using a light- sensitive channel. Nat. Methods, 4, 139–141. [PubMed: 17195846]

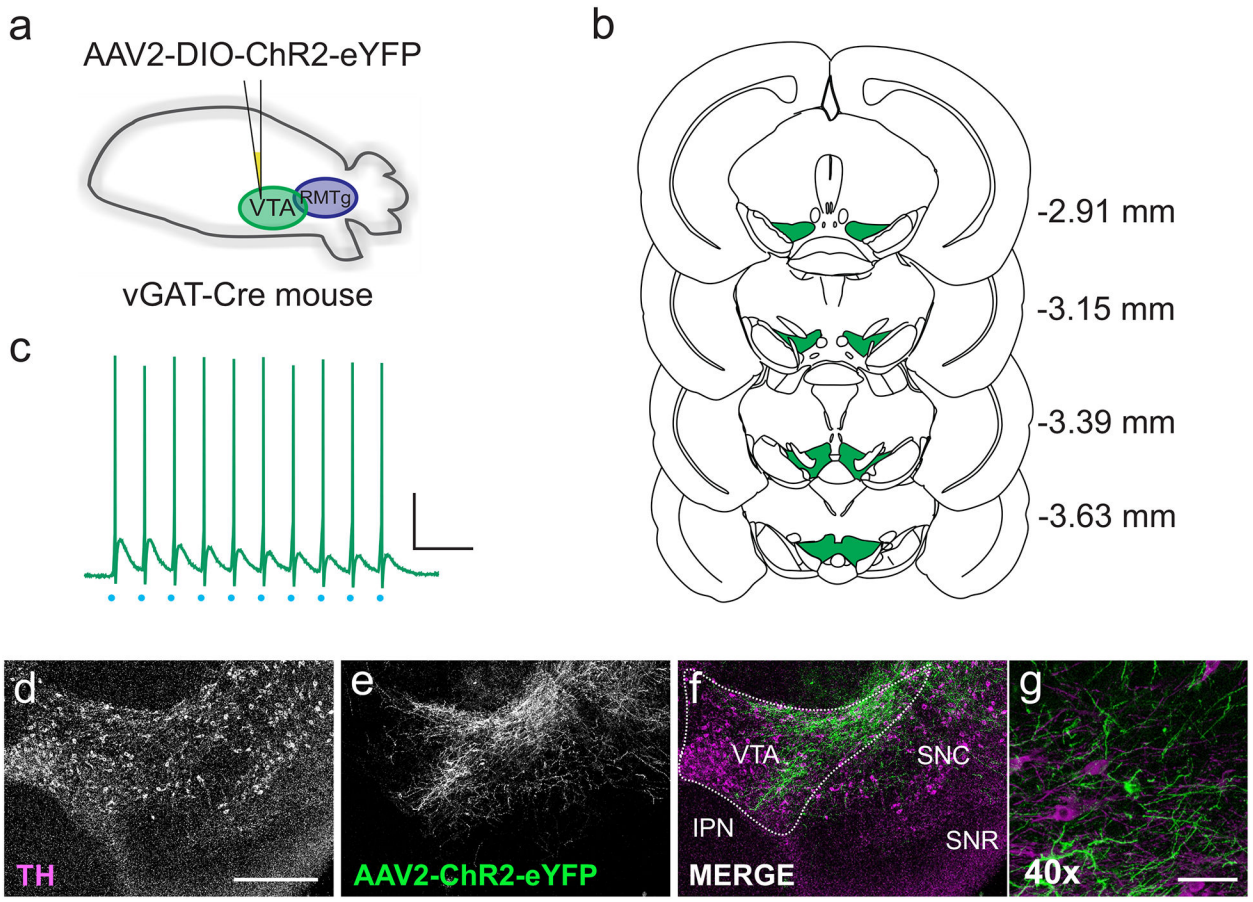

Figure 1. Isolating synaptic inputs from VTA GABAergic neurons.

(a) Schematic: VGAT- Cre mice were injected with AAV2-DIO-ChR2-eYFP into the VTA. (b) Coronal sections from 2.91 to 3.63 mm caudal to bregma, illustrating VTA extent at each level. Green area (VTA) was specifically targeted for viral injections. Coronal outlines adapted from Paxinos & Franklin, 2012. (c) Current clamp recording from a ChR2-expressing cell in the VTA. Light stimulation (blue dots) at 20 Hz elicited action potentials in the cell. Scale bar: 20 mV, 100 ms (d-g) Single coronal section through the VTA, demonstrating expression of AAV2-ChR2-eYFP 3 weeks after viral injection. (d) Tyrosine hydroxylase (TH) labels dopaminergic neurons; scale bar, 500 μm. (e) Expression pattern of AAV2-ChR2-eYFP. (f) Overlay of TH (magenta) and AAV2- ChR2-eYFP (green), showing the expression of the virus within the VTA (VTA, ventral tegmental area; IPN, interpeduncular nucleus; SNC, substantia nigra compacta; SNR, substantia nigra reticulata). (g) 40x zoom showing VTA fibers and cell bodies expressing AAV2-ChR2-eYFP (green) and TH+ cell bodies (magenta). Scale bar: 25 μm.

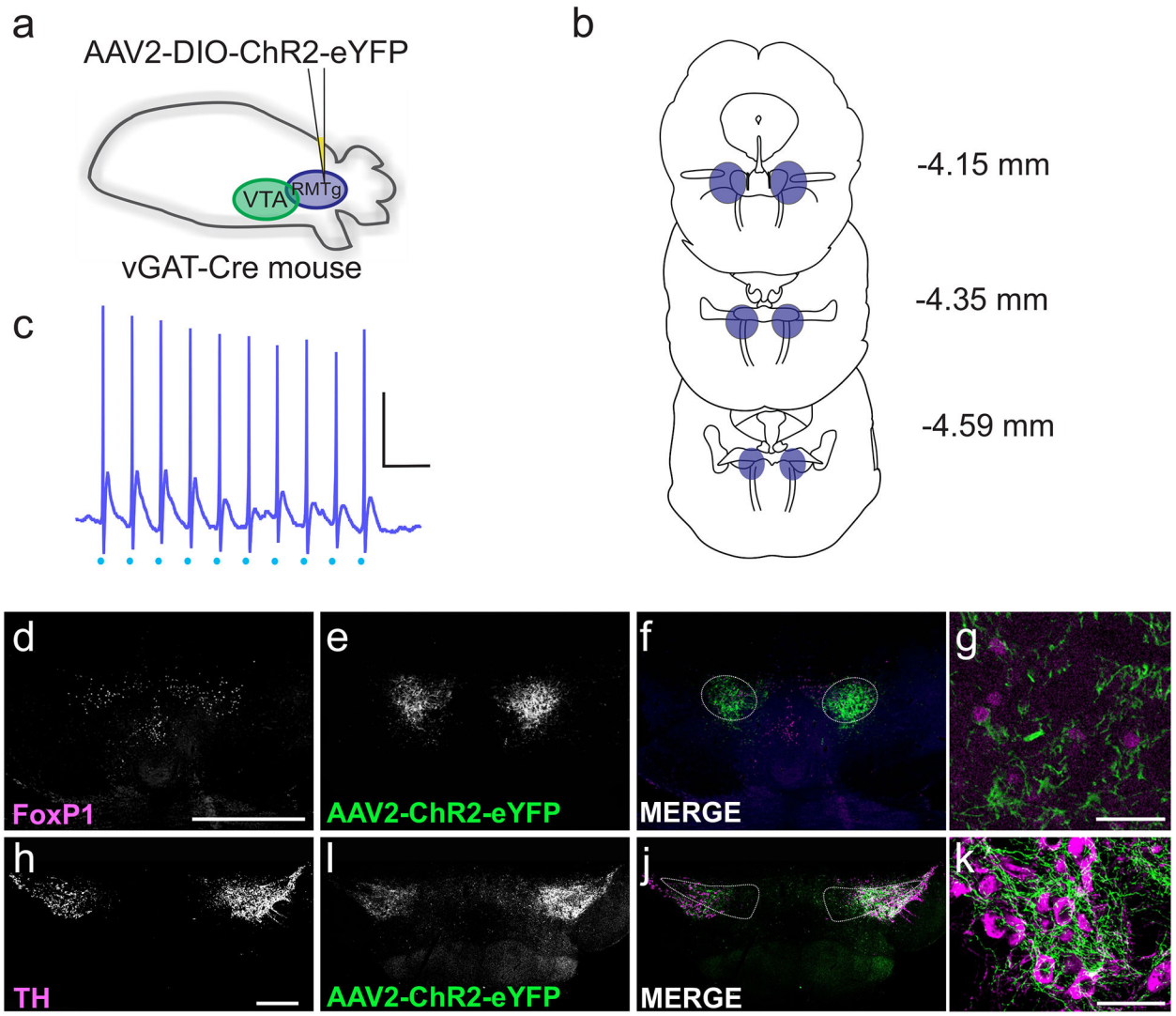

Figure 2. Isolating synaptic inputs from RMTg GABAergic neurons.

(a) Schematic: AAV2-DIO-ChR2-eYFP was injected into the RMTg (caudal to the VTA). (b) Coronal sections from 4.15 to 4.59 mm caudal to bregma illustrating the extent of the RMTg at each level; the region in blue represents the RMTg, targeted with injections. Coronal outlines adapted from Paxinos & Franklin, 2012. (c) Current clamp recording from a ChR2-expressing cell in the RMTg. Light stimulation (blue dots) at 20 Hz elicited action potentials in the cell; scale bar: 20 mV, 100 ms. (d-g) Example coronal section through the RMTg, demonstrating the expression of AAV2-ChR2-eYFP 3 weeks after viral injection. (d) FoxP1 staining identifies the RMTg; scale bar, 500 μm. (e) Expression pattern of AAV2-ChR2-eYFP. (f) Overlay of FoxP1 (magenta) and AAV2-ChR2-eYFP (green). (g) Co-labelling with AAV2-ChR2-eYFP (cytoplasmic; green) and FoxP1 (nuclear; magenta). Scale bar: 50 μm. (h-k) Example coronal section through the VTA, showing terminals from the RMTg expressing AAV2-ChR2-eYFP. (h) Immunohistochemistry for tyrosine hydroxylase (TH); scale bar, 500 μm. (i) AAV2-ChR2-eYFP in RMTg terminals within the VTA. (j) Overlay of TH (magenta) and AAV2-ChR2-eYFP (green). (k) RMTg fibers expressing

AAV2-ChR2-eYFP (green) in close proximity to TH+ cell bodies (magenta). Scale bar: 50 μm.

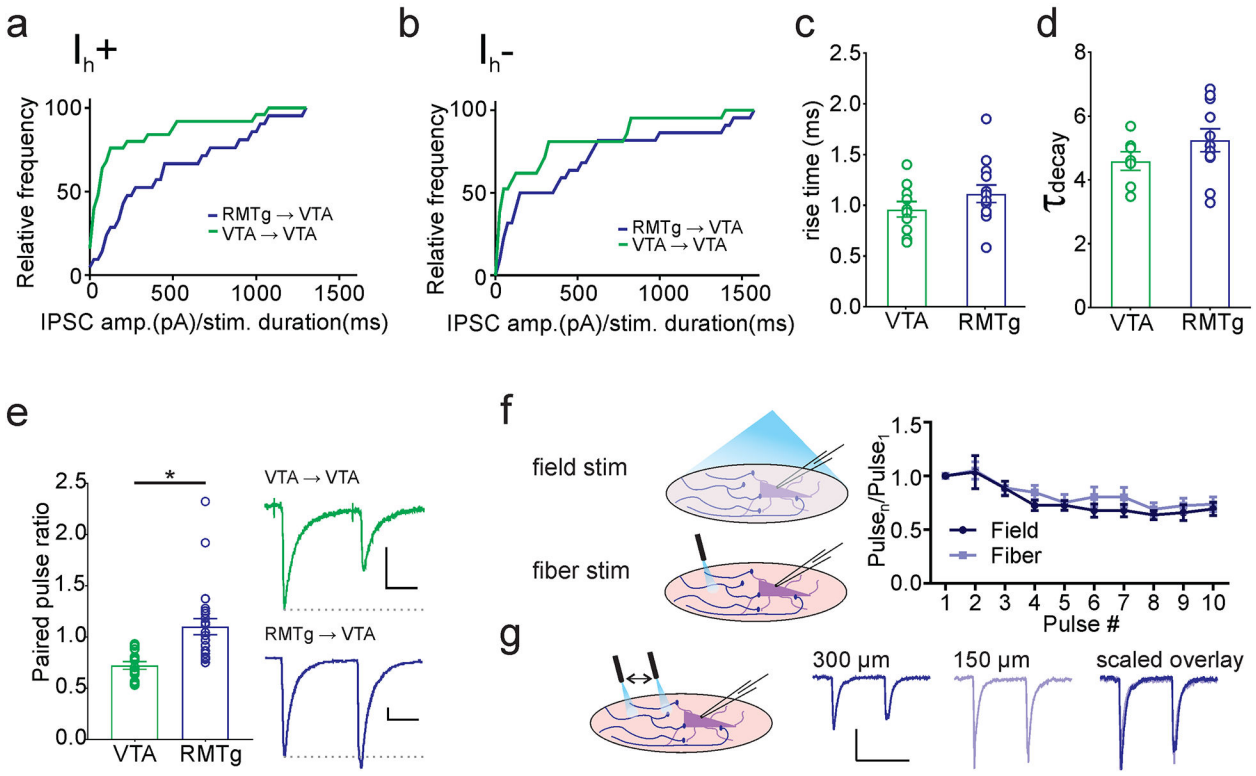

Figure 3. Basal properties of VTA→VTA and RMTg→VTA synapses.

(a) Both VTA (green) and RMTg (blue) inputs have synaptic connections with I_{h+} cells in the VTA, though on average RMTg inputs have greater IPSC amplitudes per millisecond of light stimulation (VTA inputs: n = 25 cells/23 mice; RMTg inputs: n = 21 cells/21 mice). (b) VTA neurons lacking I_h receive inputs from both regions, and also have a greater RMTg IPSC per ms light stimulation (VTA inputs: n = 21 cells/21 mice; RMTg inputs: n = 22 cells/22 mice). (c) Comparison of rise time (10–90% of peak) and decay time constant (τ_{decay}) between VTA inputs (n = 7 cells/6 mice) and RMTg inputs (n = 11 cells/9 mice). (e) RMTg inputs have a significantly greater paired-pulse ratio (PPR) than VTA inputs (* p = 0.01, Mann-Whitney U test; VTA inputs: n = 8 cells/6 mice; RMTg inputs: n = 23 cells/19 mice). Inset, paired light-evoked IPSCs from VTA (top) and RMTg (bottom). (f) Comparison of short-term depression of RMTg inputs using full-field and focal light-fiber illumination (n = 5 cells/4 mice). (g) Comparison of IPSCs elicited by a light-fiber placed at different distances from the cell body. Scale bars: 100 pA, 20 ms.

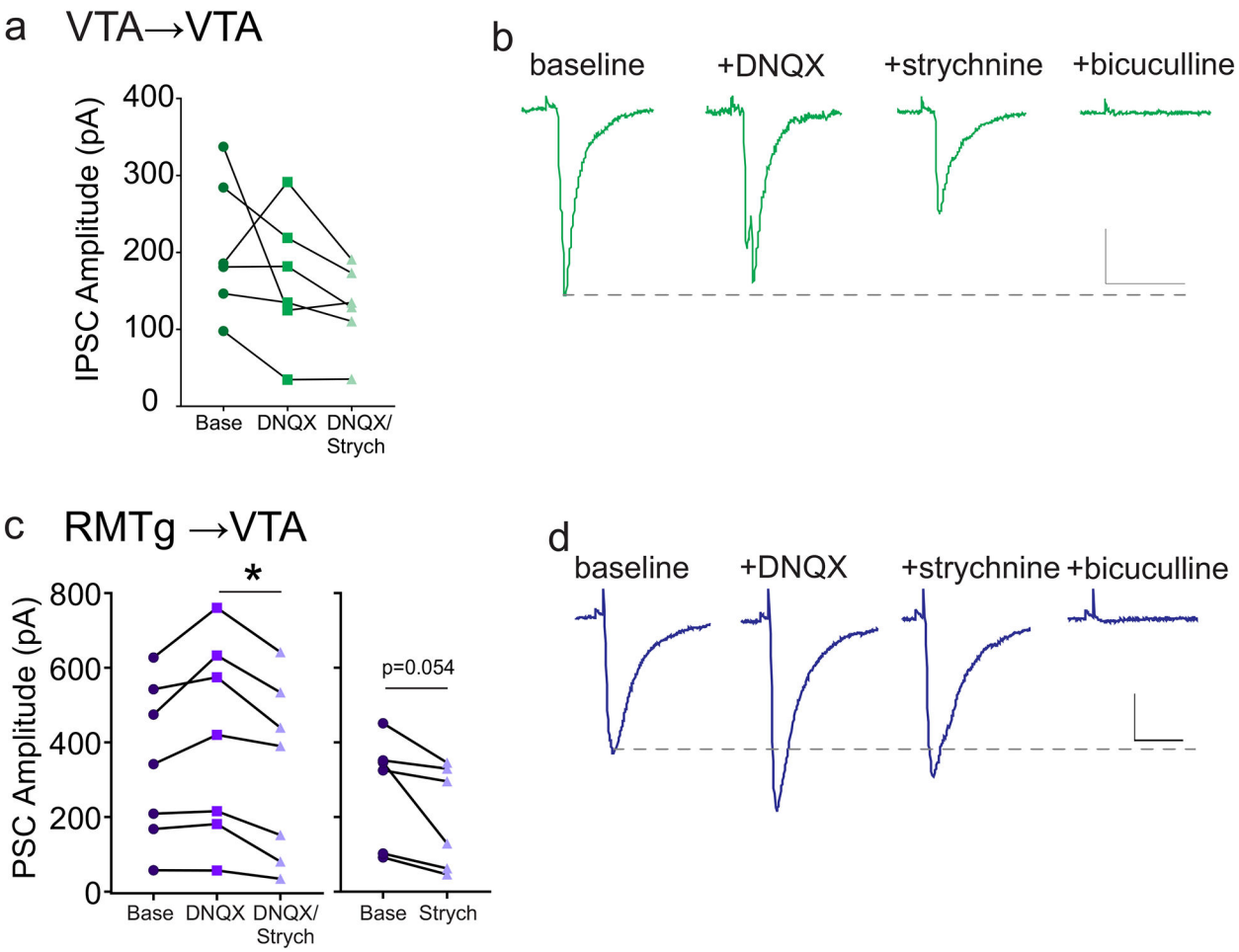

Figure 4. Neurotransmitter co-release from GABAergic terminals in the VTA and RMTg.

(a) Amplitude of light-evoked VTA→VTA PSCs were recorded before and after application of DNQX (10 μM), and then DNQX + strychnine (1 μM). (b) Representative PSCs during baseline, and during exposure to DNQX, DNQX + strychnine, and DNQX + strychnine + bicuculline (30 μM). No significant differences, 1-way ANOVA (n = 6 cells/6 mice). (c) Left panel: amplitudes of light-evoked RMTg→VTA PSCs recorded before and after application of DNQX (10 μM), and DNQX + strychnine (1 μM) (* $p < 0.05$, 1-way ANOVA; n = 7 cells/7 mice). Right panel, amplitudes of light-evoked RMTg→VTA PSCs recorded before and after application of strychnine alone (1 μM) (p = 0.05, paired t-test; n = 6 cells/5 mice). (d) Representative PSCs during baseline, and during exposure to DNQX, DNQX + strychnine, and DNQX + strychnine + bicuculline. Scale bars: 100 pA, 20 ms.

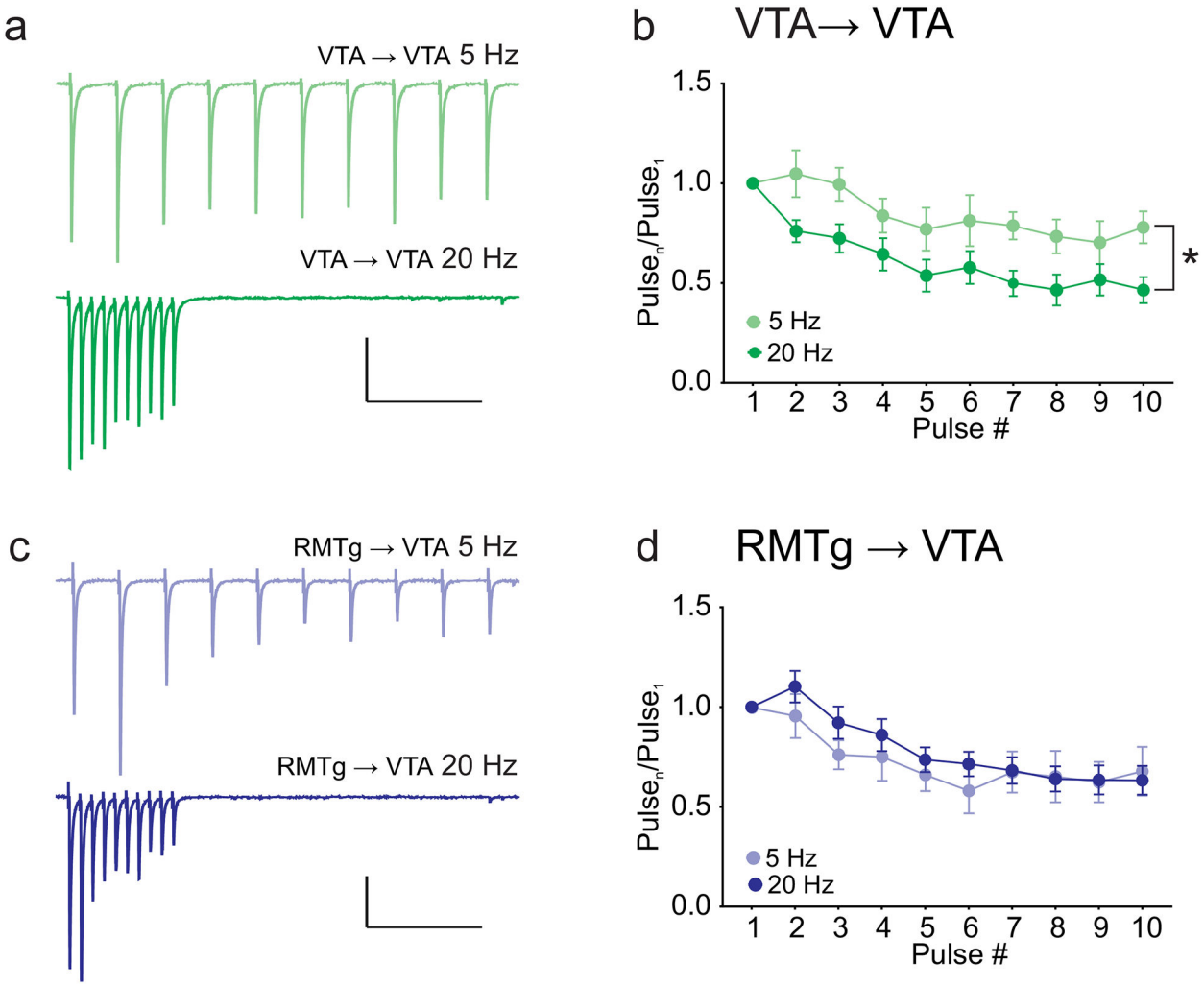

Figure 5. VTA→VTA IPSCs exhibit greater short-term synaptic depression at 20 Hz than at 5 Hz.

(a) Example IPSCs from VTA→VTA inputs evoked by trains of light stimulation at 5 Hz (top) and 20 Hz (bottom). (b) Summary of train data for VTA inputs, comparing 5 Hz and 20 Hz stimulation (* $p = 0.03$ effect of frequency, 2-way ANOVA; 20Hz: n = 8 cells/6 mice; 5 Hz n = 5 cells/5 mice). (c) Example IPSCs from RMTg→VTA inputs evoked by light stimulation at 5 Hz (top) and 20 Hz (bottom). (d) Summary of train data for RMTg inputs, comparing 5 Hz and 20 Hz stimulation. No significant effect of frequency, 2-way ANOVA (20 Hz: n = 23 cells/19 mice; 5 Hz: n = 6 cells/6 mice). Scale bars: 100 pA, 500 ms.

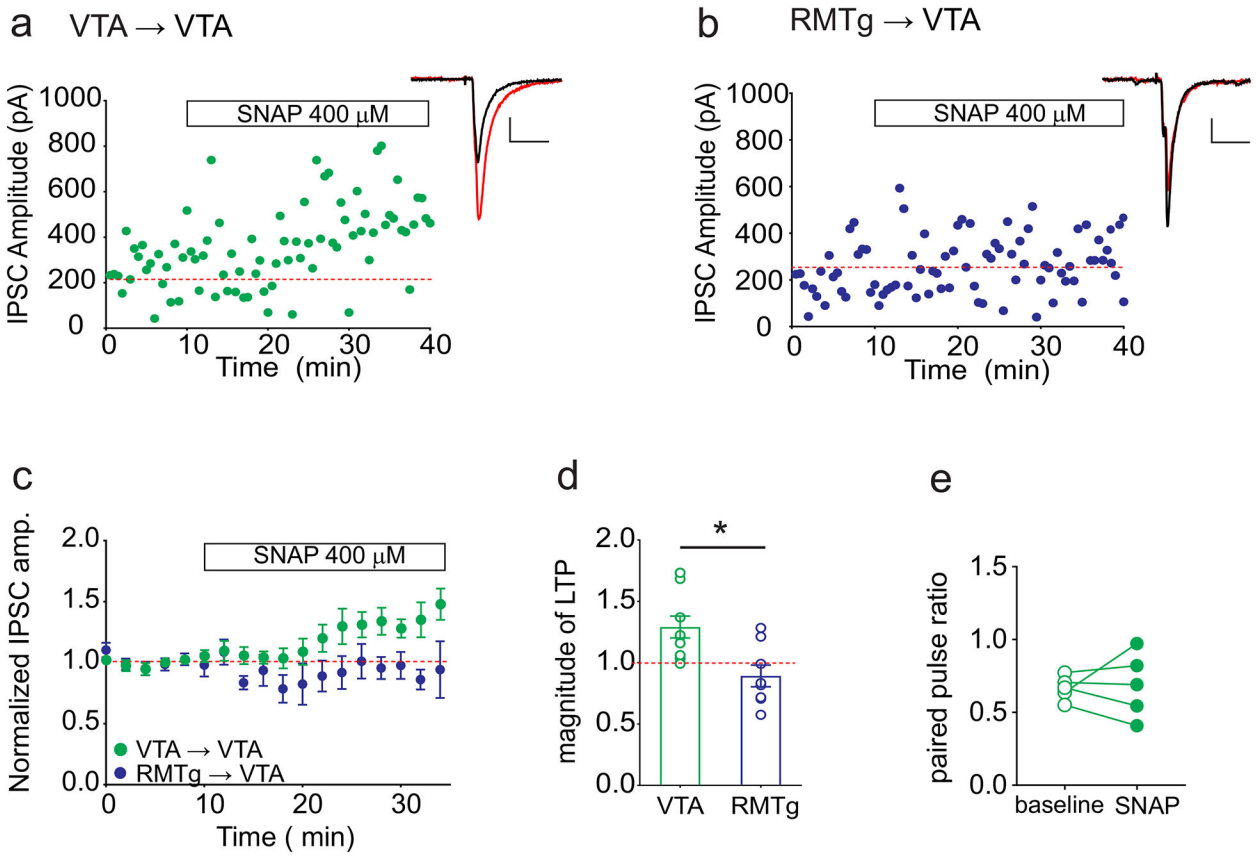

Figure 6. A nitric oxide donor potentiates light-evoked IPSCs from VTA→VTA but not RMTg→VTA inputs.

(a) Representative experiment showing LTP_{GABA} induced by application of SNAP (400 µM; white bar) during recording of light-evoked IPSCs from VTA slices. Inset: IPSCs during baseline (black) and 10–20 minutes after SNAP (red). (b) Representative experiment from mice expressing AAV2-ChR2 in GABAergic cells of the RMTg. SNAP (400 µM; white bar) application during recording of light-evoked IPSCs did not induce LTP_{GABA}. Inset: IPSCs during baseline (black) and 10–20 minutes after SNAP (red). (c) Time course of average IPSC amplitudes during treatment with SNAP for VTA→VTA and RMTg→VTA synapses. (d) Comparison of LTP magnitude at 10–20 minutes after the addition of SNAP between VTA and RMTg inputs. * $p = 0.007$, Student's t-test (VTA: n=11 cells/11 mice; RMTg: n = 8 cells/8 mice). (e) Paired pulse ratios did not significantly change for VTA→VTA inputs in cells that displayed significant potentiation (≥125% baseline). Paired t-test, $p = 0.49$, n = 6 cells. Scale bars: 100 pA, 20 ms.